



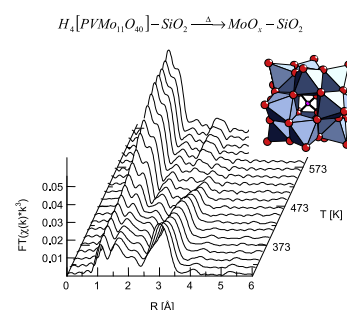
Contents

REGULAR ARTICLES

Structure and properties of $PVMo_{11}O_{40}$ heteropolyoxomolybdate supported on silica SBA-15 as selective oxidation catalyst

T. Ressler*, U. Dorn, A. Walter, S. Schwarz, A.H.P. Hahn

pp 1–10

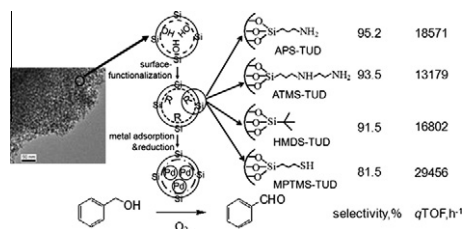


Keggin type molybdates supported on silica SBA-15 exhibited a decreased stability under selective propene oxidation conditions. The resulting active catalysts consisted of a mixture of tetrahedrally and octahedrally coordinated Mo centers.

Surface-functionalized TUD-1 mesoporous molecular sieve supported palladium for solvent-free aerobic oxidation of benzyl alcohol

pp 11–24

Yuanting Chen, Zhen Guo, Tao Chen, Yanhui Yang*

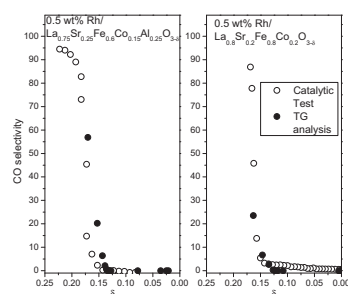


Pd supported on amino-functionalized TUD-1 catalyst shows excellent catalytic activity and selectivity in the solvent-free aerobic oxidation of benzyl alcohol, which is contributed by appropriately tuned Pd nanoparticle size and surface basicity.

Perovskite-type oxide catalysts for low temperature, anaerobic catalytic partial oxidation of methane to syngas

pp 25–33

Federica Mudu, Bjørnar Arstad*, Egil Bakken, Helmer Fjellvåg, Unni Olsbye**

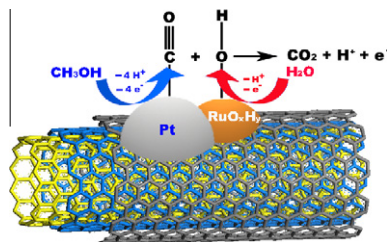


The conversion of CH_4 to CO and H_2 by the framework oxygen of perovskite oxides promoted with Rhodium was studied at 873 K. A correlation between selectivity and redox properties of the oxides was observed, suggesting a thermodynamic dependency of the products profile.

Promotion by hydrous ruthenium oxide of platinum for methanol electro-oxidation

pp 34–44

Jun-Hong Ma, Yuan-Yuan Feng, Jie Yu, Dan Zhao, An-Jie Wang, Bo-Qing Xu*

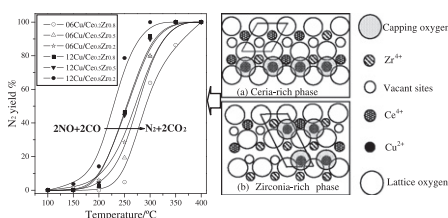


Amorphous hydrous ruthenium oxide (RuO_xH_y) alone is identified as an efficient promoter of Pt for the electro-oxidation of CO and methanol. However, its dissolution at potentials higher than 0.46 V (vs. SCE) would induce changes in Pt– RuO_xH_y proximity and even surface structure of Pt and thus alter the activity of Pt in electrocatalysis.

Correlation of structural characteristics with catalytic performance of $\text{CuO/Ce}_x\text{Zr}_{1-x}\text{O}_2$ catalysts for NO reduction by CO

pp 45–60

Lianjun Liu, Zhijian Yao, Bin Liu, Lin Dong*

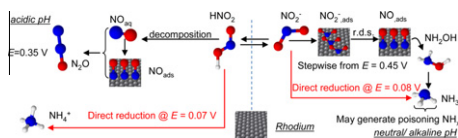


Copper species could incorporate into the vacant sites on the exposed (1 1 1) plane of ceria–zirconia, and its stronger interaction with ceria-rich phase determined the higher activity than zirconia-rich phase.

Electrocatalytic reduction of nitrite on a polycrystalline rhodium electrode

pp 61–69

M. Duca*, B. van der Klugt, M.A. Hasnat, M. Machida, M.T.M. Koper

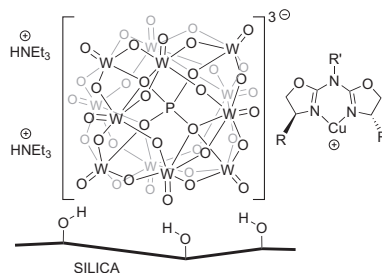


The electrochemical reduction of $\text{HNO}_2/\text{NO}_2^-$ was studied on a rhodium electrode as a function of pH and potential (E). N_2O is detected only in acidic media, while NH_3 formation occurs at low E independently of pH.

Supported heteropolyanions as solid counterions for the electrostatic immobilization of chiral copper complexes

pp 70–77

M. Rosario Torviso, Mirta N. Blanco, Carmen V. Cáceres, José M. Fraile*, José A. Mayoral**

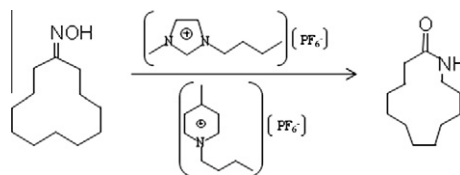


Supported ($\text{PW}_{12}\text{O}_{40}^{3-}$) is a suitable counterion to immobilize chiral azabis(oxazoline)-copper complexes by ion pair formation. Catalytic results are good to excellent in cyclopropanation reactions (up to 97% ee), with minimized leaching and good recovery after optimization of the recycling system.

In situ multinuclear solid-state NMR spectroscopy study of Beckmann rearrangement of cyclododecanone oxime in ionic liquids: The nature of catalytic sites

pp 78–83

T. Blasco, A. Corma*, S. Iborra, I. Lezcano-González, R. Montón

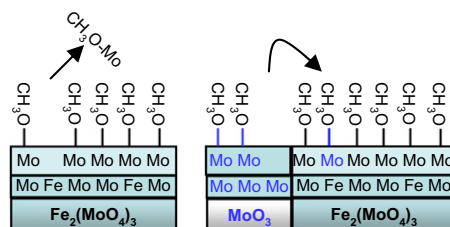


$[C_4mim]^+PF_6^-$ and $[C_4mpyr]^+PF_6^-$ ionic liquids can supply in a controlled way ppm of HF in the reaction media, which catalyze the Beckmann rearrangement of cyclododecanone oxime with excellent conversion and selectivity.

Origin of the synergistic interaction between MoO_3 and iron molybdate for the selective oxidation of methanol to formaldehyde

pp 84–98

Kamalakanta Routray, Wu Zhou, Christopher J. Kiely, Wolfgang Grünert, Israel E. Wachs*

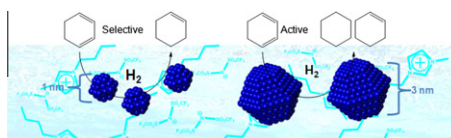


The catalytic active sites in bulk iron molybdate catalysts for methanol oxidation to formaldehyde are surface MoO_x species. The only function of excess molybdate is to replenish the volatilized surface MoO_x species. This maintains the activity and selectivity of the catalyst by preventing the exposure of iron sites responsible for yielding dimethyl ether.

Olefin hydrogenation by ruthenium nanoparticles in ionic liquid media: Does size matter?

pp 99–107

Paul S. Campbell, Catherine C. Santini*, François Bayard, Yves Chauvin, Vincent Collière, Ajda Podgoršek, Margarida F. Costa Gomes, Jacinto Sá

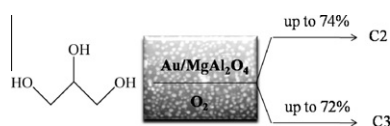


The effect of the size of ruthenium nanoparticles, produced in ionic liquids, in the catalytic hydrogenation of olefins has been investigated using 1,3-cyclohexadiene as a probe. It has been found that smaller nanoparticles are more selective, whereas larger nanoparticles present a higher activity.

Au on $MgAl_2O_4$ spinels: The effect of support surface properties in glycerol oxidation

pp 108–116

Alberto Villa, Aureliano Gaiassi, Ilenia Rossetti, Claudia L. Bianchi, Klaus van Benthem, Gabriel M. Veith*, Laura Prati**

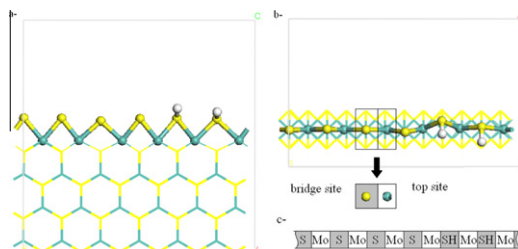


The catalytic activity of AuNPs on spinels is dependent on Au size and accessibility by the reactant, whereas selectivity is ruled out by the Mg/Al ratio at the surface.

Temperature-programmed reduction of unpromoted MoS₂-based hydrosulfurization catalysts: First-principles kinetic Monte Carlo simulations and comparison with experiments

pp 117–128

Nicolas Dinter, Marko Rusanen, Pascal Raybaud, Slavik Kasztelan, Pedro da Silva, Hervé Toulhoat*

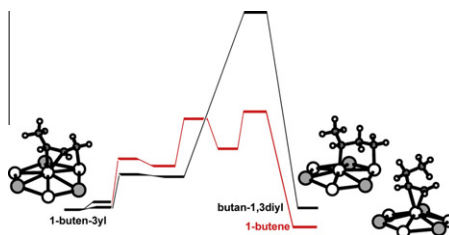


Temperature-programmed reduction profiles of pre-sulfided MoS₂/γ-Al₂O₃ hydrotreating catalysts are reproduced by first-principles kinetic Monte Carlo simulations.

Highly selective hydrogenation of butadiene on Pt/Sn alloy elucidated by first-principles calculations

pp 129–139

F. Vigné, J. Haubrich, D. Loffreda, P. Sautet, F. Delbecq*

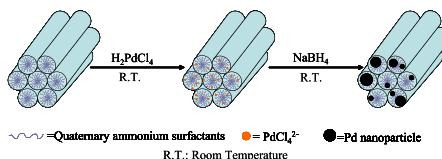


DFT calculations reveal the atomic scale mechanism of butadiene hydrogenation on a platinum-tin alloy and explain the high selectivity toward butene.

Facile preparation of supported noble metal nanoparticle catalysts with the aid of templating surfactants in mesostructured materials

pp 140–148

Hu Wang, Jin-Gui Wang, Zhu-Rui Shen, Yu-Ping Liu, Da-Tong Ding, Tie-Hong Chen*

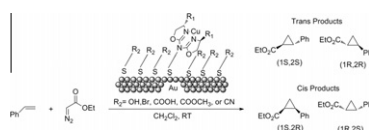


A facile method was reported to prepare as-synthesized mesostructured material supported Pd catalysts which exhibited high and stable activity in hydrogenation of allyl alcohol.

Immobilized aza-bis(oxazoline) copper catalysts on alkanethiol self-assembled monolayers on gold: Selectivity dependence on surface electronic environments

pp 149–157

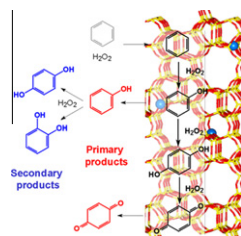
Christy C. Paluti, Ellen S. Gawalt*



Aza-bis(oxazoline) copper complex has been immobilized onto alkanethiol self-assembled monolayers utilizing five different background tail groups with different electronic characteristics.

The control of selectivity in benzene hydroxylation catalyzed by TS-1: The solvent effect and the role of crystallite size pp 158–169

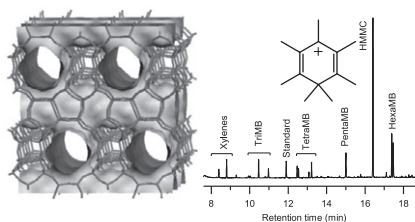
D. Barbera, F. Cavani*, T. D'Alessandro, G. Fornasari, S. Guidetti, A. Aloise, G. Giordano, M. Piumetti, B. Bonelli, C. Zanzottera



The control of selectivity in benzene hydroxylation: unraveling some controversial aspects of the catalytic behavior of TS-1. The hydroxylation of benzene with hydrogen peroxide, catalyzed by TS-1, leads to the only primary formation of phenol and benzoquinone, whereas diphenols are produced on external Ti sites and in the bulk liquid phase by consecutive phenol hydroxylation. New insights into the role of solvent and on the nature of Ti sites are also reported.

Methanol to hydrocarbons over large cavity zeolites: Toward a unified description of catalyst deactivation and the reaction mechanism pp 170–180

Morten Bjørger*, Sema Akyalcin, Unni Olsbye, Sandrine Benard, Stein Kolboe, Stian Svelle**

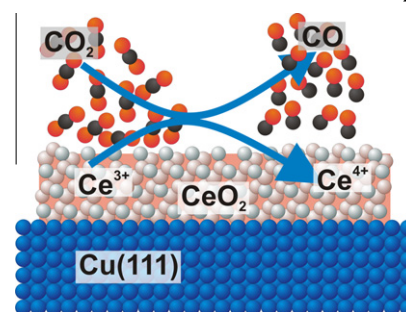


Co-reaction studies and isotopic labeling reveal profound similarities in the nature and reactivity of the reaction intermediates and the reaction steps leading to deactivation during the conversion of methanol to hydrocarbons over large cavity acidic zeolites.

RESEARCH NOTE**Ceria reoxidation by CO₂: A model study**

T. Staudt, Y. Lykhach*, N. Tsud, T. Skála, K.C. Prince, V. Matolín, J. Libuda

pp 181–185



Reduced ceria can be reoxidized by CO₂ at room temperature in complete absence of any noble metal co-catalysts, surface hydroxyl groups, or water on its surface.